Physics of the Earth and Planetary Interiors 236 (2014) 69–78

Contents lists available at ScienceDirect

Physics of the Earth and Planetary Interiors

journal homepage: www.elsevier.com/locate/pepi

Holocene paleomagnetic secular variation from East China Sea and a PSV stack of East Asia

Yan Zheng [a,c,*], Hongbo Zheng [b], Chenglong Deng [a], Qingsong Liu [a]

[a] State Key Laboratory of Lithospheric Evolution, Institute of Geology and Geophysics, Chinese Academy of Sciences, Beijing 100029, China
[b] School of Geography Science, Nanjing Normal University, Nanjing 210093, China
[c] Laboratoire des Sciences du Climat et de l'Environment/IPSL, CEA/CNRS/UVSQ, Avenue de la Terrasse, 91198 Gif-sur-Yvette cedex, France

ARTICLE INFO

Article history:
Received 10 April 2014
Received in revised form 24 June 2014
Accepted 2 July 2014
Available online 14 July 2014

Keywords:
Paleomagnetic secular variation
The Holocene
PSV stack
East China Sea
East Asia

ABSTRACT

Paleomagnetic secular variation (PSV) provides information on the mechanisms of the geodynamo and can also be used for stratigraphic correlation on a regional scale. In this study, we constructed PSV curves of relative rapidly deposited Holocene marine sequence from East China Sea. Results show that the dominant magnetic carriers are pseudo-single domain (PSD) to multidomain (MD) magnetites. Paleomagnetic directions are preserved by coarse-grained magnetite, even affected by post-depositional diagenetic alteration. The PSV record of core MD06-3040 exhibits six major inclination peaks and five declination swings during the Holocene. The periodicities for inclination are about 2000 and 550 years, and for declination are about 1400 and 500 years. The PSV of MD06-3040 is comparable to archeomagnetic and historic results for the last 2500 years and to PSV results from lake sediments in southern China and Japan during the Holocene. A PSV stack of East Asia is constructed by sedimentary and archeological PSV results, which can be used as an important reference curve for a large region, and the PSV correlation between sites can be applied for relative dating of East Asia.

1. Introduction

Paleomagnetic secular variation (PSV) originates from changes in the flow patterns in the liquid outer core of the Earth. For the last 400 years, PSV data were recorded by historical observations (e.g. Jackson et al., 2000; Lhuillier et al., 2011; Demetrescu and Dobrica, 2014). Archeological materials (e.g. hearths, kiln, etc.) (e.g. Yang et al., 2000; Hervé et al., 2013; Cai et al., 2014), as well as lake and/or marine sediments with high sedimentation rates (e.g. Yang et al., 2012; Lougheed et al., 2012) have been utilized to characterize the magnetic field variations on millennial scales. Among these PSV recorders, sediments could provide continuous results, and with high-resolution, which could not be obtained from volcanic and archeological materials.

Continental PSV record could originate from lacustrine sediments, which have been widely carried out on cores from lakes in North America (e.g. Lund, 1996; Brachfeld and Banerjee, 2000; Barletta et al., 2010) and Europe (e.g. Ojala and Saarinen, 2002; Clelland and Batt, 2012). Then, PSV stacks were produced from these regional records (Ojala and Tiljander, 2003; Snowball et al., 2007), which were used as reference curves for dating on Holocene sediments. In this context, PSV records from East Asia are still relatively sparse (Hyodo et al., 1999; Yang et al., 2009; Yang et al., 2012; Ali et al., 1999), so there is no PSV stack in this area. In contrast with continental records, directional (declination and inclination) PSV records from marine sediments are relatively scarce (e.g. Lougheed et al., 2012; Stoner et al., 2007; Heirtzler and Nazarova, 2003). Therefore, paleomagnetic directional study was carried out on high sedimentation rate core MD06-3040 (27°43.4′N, 121°46.9′E) from the East China Sea continental shelf, which provides an excellent interpretative background on rock magnetic study previously (Zheng et al., 2010). In this paper, we aim to obtain PSV records of core MD06-3040, and then analyze the patterns of East Asia and further construct PSV stack of East Asia.

2. Study area and core descriptions

Previous studies in East China Sea have revealed an elongated (~800 km) distal subaqueous mud wedge extending from the Yangtze River mouth southward along the Eastern China coasts into the Taiwan Strait (e.g. Qin et al., 1987). Most of the sediments in the mud wedge originate from the Yangtze River, with much smaller (<1%) input from smaller local rivers (e.g. Liu et al., 2007). The East China Sea continental shelf was subaerially

* Corresponding author. Present address: Institute of Vertebrate Paleontology and Paleoanthropology, Chinese Academy of Sciences, Beijing 100044, China.
E-mail addresses: zy99413@gmail.com, zhengyan@ivpp.ac.cn (Y. Zheng).

http://dx.doi.org/10.1016/j.pepi.2014.07.001
0031-9201/

exposed during the Last Glacial Maximum (LGM), and this mud wedge along the shore is mainly formed during the Holocene (e.g. Liu et al., 2007) (Fig. 1).

During the IMAGES XIV-MD155-Marco Polo 2 cruise of the R.V. *Marion Dufresne* in 2006, calypso core MD06-3040 was recovered from the mud wedge off the coast of Zhejiang province on the East China Sea inner continental shelf (27°43.4′N, 121°46.9′E; Fig. 1) at a water depth of 46 m. This calypso core is 19.22 m long and penetrates through the base of the mud section (Laj et al., 2006) into the sand of LGM age. The lower part of the core (below 18.5 m) contains interbedded with sands and silts which were formed during LGM and early Holocene transgression, while sediments between 15.8 and 18.5 m consist of silt clay, and the top 18.5 m sediments are composed of clays (Zheng et al., 2010). Here, we'd like to do paleomagnetic research on the upper 18.5 m sediments.

3. Experimental methods

Measurements of the low-field magnetic susceptibility and remanent magnetizations were performed on U-channel samples at the Laboratoire des Sciences du Climat et de l'Environment (LSCE). The magnetic method and measuring sequences on U-channel samples are described in details by Zheng et al. (2010).

In order to determine the low temperature magnetic phase transitions characteristic of magnetic minerals, we performed measurements using the Quantum Design MPMS 5 magnetic properties measurement system at the Paleomagnetism and Geochronology Laboratory (PGL), Institute of Geology and Geophysics, Chinese Academy of Sciences (IGG-CAS) in Beijing. Dried 0.04–0.1 g subsamples were cooled in zero-field down to 10 K when a remanence was imparted in a field of 2.5 T. The field was then removed and the behavior of the remanent magnetization was measured upon heating from 10 to 300 K. This experiment will be labeled Zero Field Cooled (ZFC) experiment.

Magnetic extracts for Scanning Electron Microscope (SEM) were obtained from dry bulk sediments. About 1 g of sediment was dispersed by ultrasonic agitation in ethanol. No additional chemical treatment was performed on the samples prior to magnetic extraction to avoid any alteration effects. The extraction was made by passing the sample into the poles of a magnet and it took about 0.5–1 h per sample. The extraction was stopped when visible gain in material was no longer achieved. Magnetic extract particles were fixed onto a carbon sticker, previously stuck on a standard stub, and then were coated with a carbon layer of a few nm to prevent surface charging of the sample during SEM operation. All SEM analyses were performed using LEO-1450 VP at 15 kV acceleration voltages at IGG-CAS, Beijing. Backscattered electron (BSE) modes were used for imaging and energy dispersive X-ray spectroscopy (EDS) for elemental composition.

4. Results

4.1. Core stratigraphy

Age model for calypso core MD06-3040 is based on AMS ^{14}C dates of bivalve shells from CASQ core MD06-3039 (8.1 m) nearby and core MD06-3040 (below 8 m). Stratigraphic correlation between the two cores is according to their similar magnetic susceptibility records (Appendix Fig. 1). Based on the susceptibility and other sediments physical features, we suggest that the uppermost 1.8 m of core MD06-3040 is stretched during coring process (Skinner and McCave, 2003), which corresponds to the top 1 m of MD06-3039, while the sediments below 1.8 m of core MD06-3040 are not stretched or shortened. Ages from the two cores indicate that core MD06-3040 spans the entire Holocene (Zheng et al., 2010) (Fig. 2d). The average sediment accumulation rate was estimated to be approximately 2 mm/year, and therefore the theoretical temporal resolution of magnetic analyses is about 20-year (Zheng et al., 2010). As coarse-grained sediments are not suitable material for paleomagnetic studies, the uppermost 18.5 m sediments (clay and silt clay) of core MD06-3040 are considered here.

4.2. Rock magnetism

The main rock-magnetic variations in this core and their paleoclimate implications have been discussed by Zheng et al. (2010) and a summarized plot on the down-core rock-magnetic variations is presented in Fig. 2, from which some basic magnetic information could be obtained. Magnetic concentration is lower in the lower part (below 9 m) than that in the top part (above 8.45 m), and magnetic grains are coarser in the bottom part than that at the top part. Except the extreme high coercivity zone at about 8.45–9 m, magnetic minerals are softer in the top part, which indicates the high contribution from magnetite in the sediments that above 8.45 m.

In order to distinguish the magnetic minerals, ZFC remanence measurements and SEM observations are made (Figs. 2 and 3). Magnetite can be recognized by ZFC remanence curves in the whole core (Fig. 2 on the right side), which confirms that a significant fraction of the magnetite are still well preserved after reductive diagenetic process, consistent with the conclusion drawn by Yamazaki et al. (2003) on a Pacific core. The Verwey transition at 120 K are much clearer in the lower samples than in the upper

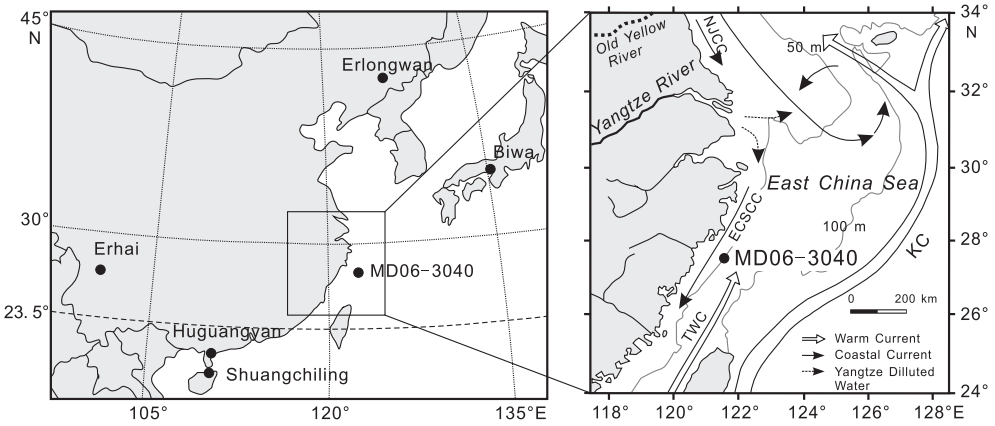

Fig. 1. Schematic map of East Asia with locations where lacustrine PSV obtained and detailed information about East China Sea continental shelf, where the studied core MD06-3040 drilled.

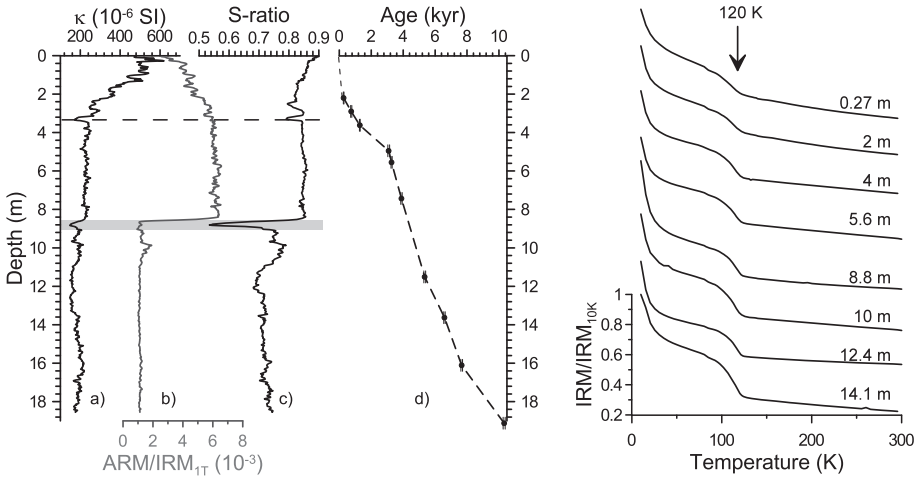

Fig. 2. Down-core variation of rock-magnetic parameters on the left, κ (a), ARM/IRM_{1T} (b), and S-ratio (c), as well as the age-depth model (d) for core MD06-3040 (summarized from Zheng et al., 2010). Zero-field cooled (ZFC) remanence (imparted in a field of 2.5 T at 10 K) on warming for eight subsamples from 10–300 K are shown on the right.

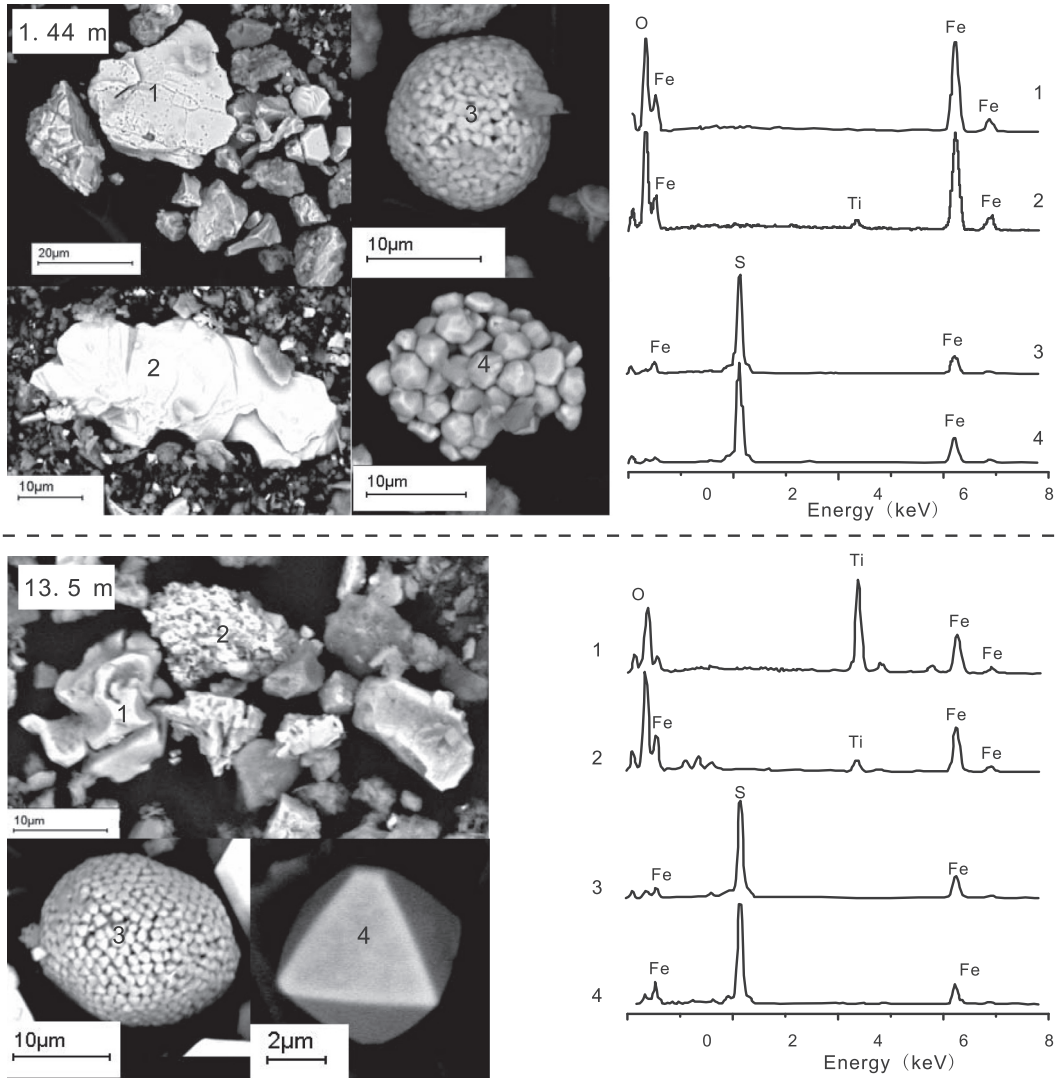

Fig. 3. Scanning electron microscopy graphs in Backscattered electron (BSE) mode with elemental spectra for sediments at depth of 1.44 m and 13.5 m of core MD06-3040.

samples, indicating that there might be larger contributions from MD magnetite to IRM in the bottom samples (Smirnov, 2006). This supports the down-core variation of ARM/IRM_{1T} (Fig. 2b), which we interpret as a decrease in the amount of fine SD and PSD magnetite below 8.45 m (Zheng et al., 2010).

From SEM observation, iron oxides and iron sulfides are identified in magnetic extraction samples from both the upper and lower part sediments (Fig. 3). Irregular shape particles are mainly composed of Fe and O, and some particles contain Ti. The atomic ratios of Fe (Ti) and O are about 2:3, 3:4, or 1:1, which indicates that these iron oxides are mostly (titano-)magnetite and/or hematite. The grain sizes of these iron oxides in the sample at 1.44 m depth are distributed from several micrometers to over 30 μm, but only coarse grains (about 10–30 μm) exist in the sample at depth of 13.5 m. This is consistent with the low temperature magnetic results that more coarse magnetic grains in the bottom part (Fig. 2 right plots).

Particles with regular shape are composed of Fe and S, and atomic ratios of Fe and S are very close to 1. Round cluster of iron sulfide in the sample at 1.44 m is about 10 μm and only a tiny amount of total magnetic grains (about 10%). Iron sulfides in the sample at 13.5 m present round clusters (~10 μm in diameter) and also regular octahedral grains (~2–10 μm in diameter) with a considerable amount of total magnetic grains (50–60%). Canfield and Berner (1987) pointed out that clusters grains in sediments after diagenetic alteration were look like pyrite spherules but with magnetite core. As the samples for SEM were obtained by magnetic extraction, we suppose that regular octahedral shaped iron sulfides are most probably greigite formed post- or syn-deposition, which has stronger magnetism than other iron sulfides. The clusters grains should be pyrite spherules with a relatively large magnetite core. The SEM observation results are consistent with the κ–T measurements that there are more iron sulfides below 8.45 m (Zheng et al., 2010), but magnetite are also preserved after diagenetic alteration.

These new investigations confirm that the sedimentary sequence from East China Sea can be separated into two main parts: part I (0.15–8.45 m), magnetic characteristics are characterized by fine PSD magnetite grains, some hematite and some iron sulfide; part II (9–18.5 m), magnetic characteristics are characterized by coarse (PSD + MD) magnetite grains and more iron sulfide, such as greigite and/or pyrite. The part between part I and II (8.45–9 m) is a transitional zone of the two obvious different magnetic component units, which is composed by high concentration of high coercivity magnetic minerals. Existence of coarse-grained magnetite down-core indicates less impacted by post-depositional activities.

4.3. Paleomagnetic demagnetization and directional record

Demagnetization behaviors on end-point projection diagrams and NRM decay diagram upon are shown in Fig. 5. End-point projection diagrams (Zijderveld, 1967) reveal that, except for the very first steps, the data points lie on a straight line trending to the origin, indicating that a single stable component of magnetization is individualized (Fig. 4). For samples from sediments above 8.45 m (part I), NRM and ARM present similar demagnetization features, and both reach a value close to zero at 80 mT which marks the end of the AF demagnetization (Fig. 4). On the contrary, NRM and ARM show different demagnetization behaviors below 9 m (part II). Samples from 8.79 m and 14.1 m could not be entirely demagnetized at 80 mT, and the NRM_{80mT} of samples from 8.79 m is still 20% of the NRM_{0mT}. ARM in part II are harder to demagnetized than NRM (Fig. 4), which indicate less contribution from SD magnetite in this part as ARM is very sensitive to SD magnetite than other parameters. Medium destructive field (MDF) down-core variations (Fig. 5f) also present that the coercivity of part II is smaller than that of part I, which is also due to the high concentration of MD magnetite grains in part II. This is consistent with the rock-magnetic analyses of this core (Fig. 2, Zheng et al., 2010).

After principal component analysis (PCA), the inclination and declination values of the Characteristic Remanent Magnetization (ChRM) could be obtained (the number of steps for AF demagnetization considered for PCA analysis varies between 8 and 12). Inclination varies about an average value of 46.4° (dashed line in Fig. 5b), which corresponds to the expected GAD inclination of 43° at 27.7° latitude. This supports that the PSV record is reliable. Noticeable eastward trend with depth of declination values likely result from a regular twisting of the corer during the coring process, which has to be accounted for (dashed line in Fig. 5c). A corrected declination was obtained after removing this trend (Fig. 5d). The stability of paleomagnetic record upon demagnetization and the accuracy with, which the directions of the ChRM are defined, is given by the maximum angular deviations (MAD), which does not exceed 8° and 95% of them are less than 5° (Fig. 5e). Paleomagnetic data of this study are convincible.

5. Discussion

5.1. PSV features of East China Sea

The top 70 cm of core MD06-3040 is characterized by high water content, so the large changes in declination/inclination observed at the top part (Fig. 5b and d) of the core is considered to be perturbations and consequently not discussed below. Given the susceptibility comparison between core MD06-3040 and core MD06-3039, the uppermost 1.8 m sediments of core MD06-3040 are stretched during drilling processes (Appendix Fig. 1), so directional results should be also somewhat suffered from the coring process. On the PSV of core MD06-3040 versus time (Fig. 6), the upper 1.8 m corresponds about the last cal. 200 years, we prefer to show the PSV between 0.7 and 1.8 m on the plot, but do not discuss two much. Several long-term changing features of inclination and declination on core MD06-3040 are recognizable, which could be used as relative dating reference curves for East China Sea (Fig. 6).

Inclination varies around the expected GAD inclination of 43° at 27.7° latitude, and presents six major inclination peaks. The first inclination peak (No. 1) consists of two major peaks and one minor peak between, and the changing amplitude is about 20°. The second peak (No. 2) is shown as three minor peaks (changing amplitude is less than 10) and the third one (No. 3) is composed of two main small peaks, but last longer than those small peaks of second peaks. An increasing trend on the inclination profile of the second and third peaks (5–1.5 ka) is also observed (Fig. 6). The other three peaks (Nos. 4, 5 and 6) are all composed by one major peak and with some small peaks between them. The fluctuation amplitude of the six inclination peaks is bigger than the others, which is possible due to more contribution from silts in the sediments (Zheng et al., 2010).

Declination of core MD06-3040 shows simple changing pattern, with five obvious major eastward swings. The first declination eastward swing (No. 1′) consists of three peaks, and the youngest peak lasts less than 100 years. The second eastward swing (No. 2′) is minor, with amplitude of only 20°, which lasts about 1.5 ka (~1.5–3 ka). The third eastward swing (No. 3′) is the major one, with about 40° changes and lasting 2.5 ka. From the ~5 ka to ~1.5 ka, the declination presents a westward trend. The fourth one is composed of four minor changes, with a declination eastward trend from ~8.5 ka to ~ 6 ka. In this case, the eastward

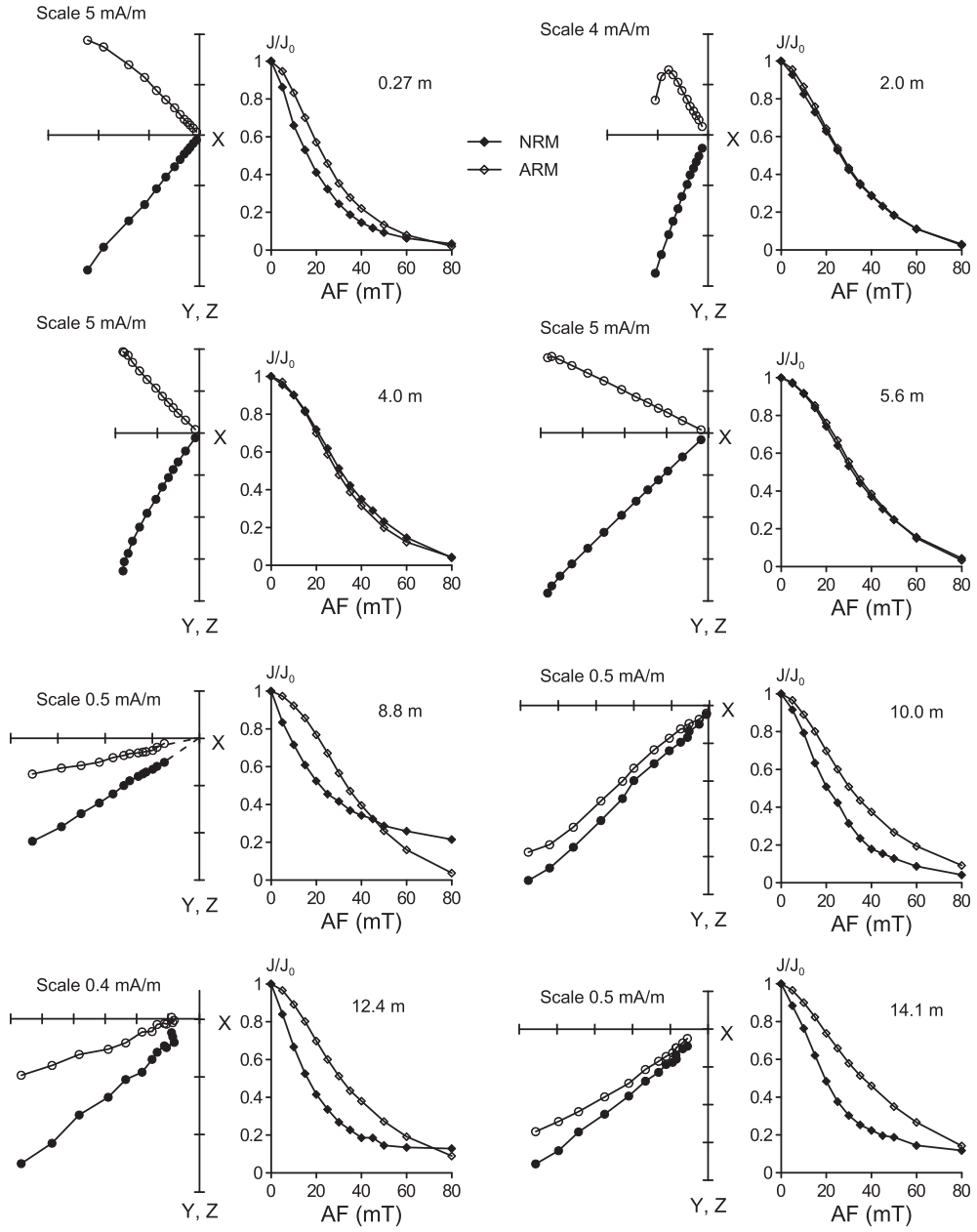

Fig. 4. Vector end-point diagrams of stepwise AF demagnetization of NRM, and normalized decay curves (depths are shown at right up corner of each plot). Demagnetization steps are: 0, 5, 10, 15, 20, 25, 30, 35, 40, 45, 50, 60, and 80 mT. Solid and open circles represent NRM projections onto vertical and horizontal planes, respectively. Solid and open diamonds represent NRM and ARM demagnetization respectively. Note that declinations are uncorrected.

swings 2, 3 and 4 could also be recognized as a major swing in long-term. The fifth swing shows declination changes of over 50°, and lasts 1.5 ka (10–8.5 ka). This big change coincides with the big variation of inclination (peak 6), which are possibly caused by the coarser sediment grains at this interval.

Power spectrum of inclination and declination records was further analyzed by Redfit software (Schulz and Stattegger, 1997). Inclination data show major peaks at periodicities of about 2000 and 550 years, and declination data show periods at about 1400 and 500 years. The similar spectral power at period for PSV results have been previously reported (Gogorza et al., 2000; St-Onge et al., 2003).

5.2. PSV comparison of East Asia

In order to establish the regional significance, we compared our PSV with previous paleomagnetic results. Given the geographic location of core MD06-3040, PSV data from China and Japan are chosen to be compared. Firstly, we compare our result with published archeomagnetic PSV results from China and Japan compiled in GEOMAGIA 50 database (Korhonen et al., 2008), as well as sedimentary and historical records of observation from Japan (Hyodo et al., 1999). Since there are scare data before 2.5 ka, here we prefer to do archeomagnetic PSV comparison for the last 2500 years (Fig. 7). There are also Then PSV of East China Sea was compared with those lake PSV results, from and Biwa Lake in central Japan (Ali et al., 1999), Erlongwan in northeastern China (Frank, 2007), Huguangyan (HGY) Lake (Yang et al., 2012) and ShuangChiLing (SCL) Lake in southern China (Yang et al., 2009) and Erhai Lake in southwest China (Hyodo et al., 1999) (Fig. 8, locations of these sedimentary cores are shown in Fig. 1). All these PSV comparisons are based on the features both on inclination and declination together.

In Fig. 6, two major peaks of inclination from China could be observed between 1 and 2 ka, and two troughs could be recognized

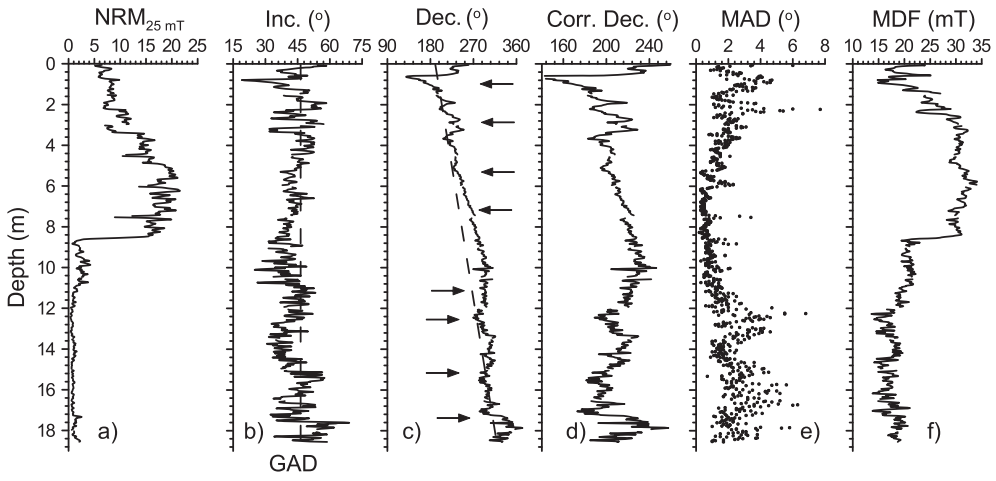

Fig. 5. Down-core variations of NRM_{25mT} (a), and inclination (b), declination (c), corrected declination (d), maximum angular deviation (MAD) (e), and Medium destructive Field (MDF) (f) after principal component analysis (PCA). Dashed lines in b and c profiles represent expected GAD inclination at 27.7° latitude and secular twisting linear trends, respectively.

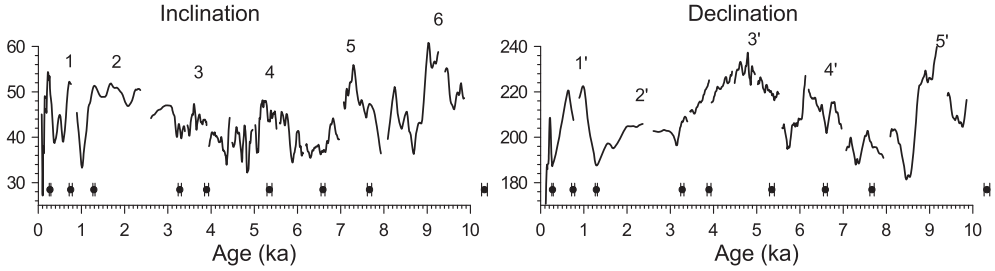

Fig. 6. PSV of MD06-3040 (after smoothing of 9 points) against timescale, with numbers representing obvious inclination peaks and eastward declination swings.

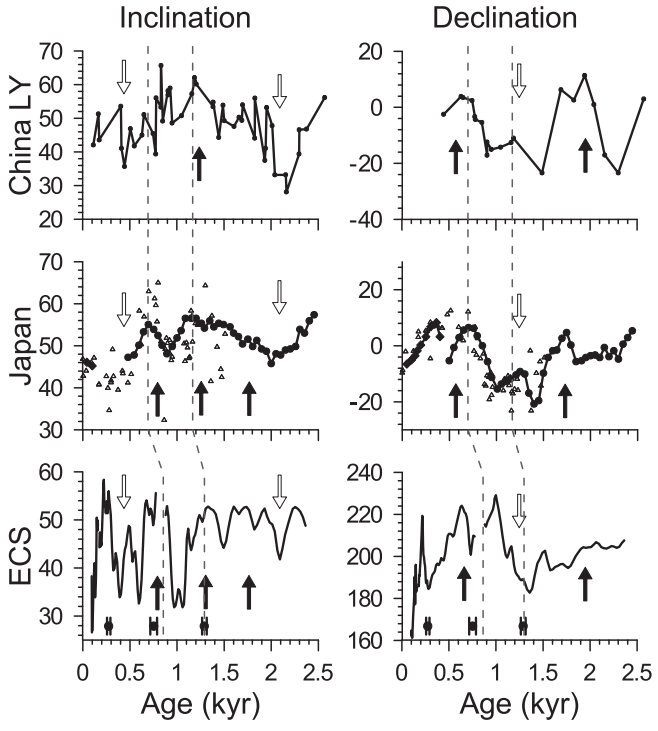

Fig. 7. Comparison of the PSV of core MD06-3040 to published archeological data compiled in GEOMAGIA (Korhonen et al., 2008) from central China and Japan (triangles) of the last 2000 years. Paleomagnetic results from sediment (solid circles), historical records of observation (solid diamonds) from Japan are also shown (Hyodo et al., 1999). Calibrated ^{14}C ages and dating errors of MD06-3040 are shown below PSV curves (dots and error bars).

around 0.45 ka and 2.1 ka. There are also two inclination troughs from Japan, and one of them matches the trough around 0.5 ka, and another one around 2.3 ka, while three troughs are recognizable among these peaks. All these inclination peaks and troughs features (arrows in Fig. 7) that observed from archeomagnetic data could be found on inclination curves from East China Sea, but in different changing amplitudes. This continuous data of East China Sea provide more detailed information.

The declination data of China archeomagnetic results presents similar variations from Japan. One obvious westward swing is observed at about 1–1.4 ka from both China and Japan, while eastward swings are shown on the part younger than 1 ka and older than 1.4 ka (arrows in Fig. 7). The westward swing of core MD06-3040 is abrupt and only last one hundred years, which is shorter than that observed from archeomagnetic results. Considering the well compared inclination between these data (Fig. 7), the difference declination behavior could be possibly due to some local effects. Consequently, we suppose that the sedimentary PSV from East China Sea is comparable to those archeomagnetic PSVs data.

PSV comparison between marine sediments (this study) and lakes from China and Japan is shown in Fig. 7. PSV of Biwa, Erlongwan and HGY are composite results of the lakes, some noise were eliminated by the combining process. PSV data of MD06-3040 and SCL, however, were obtained from one core, so a 9-point smoothing was applied to the PSV data of MD06-3040 and SCL Lake, to enhance the signal/noise ratio, and reduce high frequency scatter. Age controls (with error bars) of each PSV also exhibit under the curves. Age models for these studies are based on radiocarbon dating, but dated materials and calibration methods are different. And there is no calibration on ^{14}C ages of Erhai Lake. In order to minimize the differences caused by calibration, ^{14}C ages

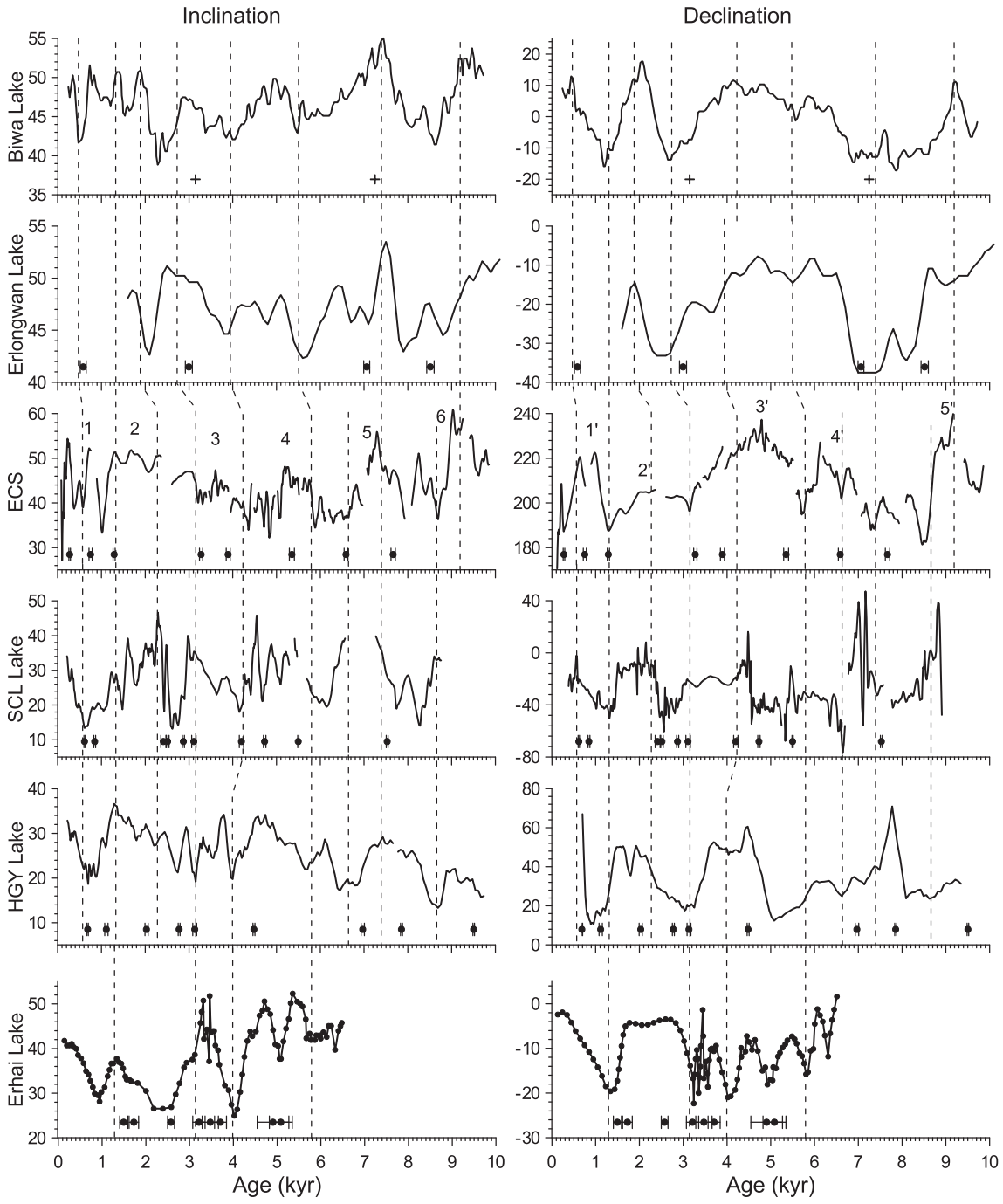

Fig. 8. Comparison of the Holocene PSV records of core MD06-3040 to other sedimentary PSV results from Biwa Lake (Ali et al., 1999), Erlongwan (Frank, 2007), ShuangChiLing (SCL) Lake (Yang et al., 2009), HuGuangYan (HGY) Lake (Yang et al., 2012) and Erhai Lake (Hyodo et al., 1999) in south China, with correlation lines (dashed lines) between them, based on features of both inclination and declination.

of HGY, SCL and Erhai Lakes are calibrated by Calib602 (Intcal09 curve) before PSV comparison. MD06-3040 locates just in the center of these cores, so the comparison between MD06-3040 and Biwa, Erlongwan Lakes from northeast part would be done first, and comparison to SCL, HGY and Erhai from south and southwest would be done latter.

PSV of MD06-3040 presents similar variations to that of Biwa Lake from 10 ka to 3 ka. Inclination of the last 3 ka shows more detailed variations than that of Biwa Lake. Based on the declination changing pattern, two correlation lines are built for the last 1.5 ka, which are also suitable for the inclination. Then, the PSVs of Biwa and MD06-3040 are suggested to share the same changing behavior. PSV of Erlongwan core, from northeast China, is also share the similar pattern to that MD06-3040 and Biwa Lake present.

SCL Lake presents some differences variations from the MD06-3040, but some similarities could be also found between them. The inclination peaks 2, 3 and 4 of core MD06-3040 could be found on the SCL inclination curve, and the declination swings 2, 3 and 4 could be partially compared. We conclude that some of the PSV features of SCL Lake are comparable to that of MD06-3040, but in different amplitude. However, the inclination of SCL Lake is low between 2.5 and 3 ka and a decreasing trend from 2.3 to 0.5 ka, which is not observed from other sites. We suppose that the inclination of SCL of this part might be some local signals.

HGY Lake, another PSV results from southern China, shares same inclination variations with MS06-3040 between 1.3 and 5.8 ka, also showing similar changes to SCL Lake since 1.3 ka. The inclination peaks 5 and 6 of MD06-3040 could be observed in the HGY Lake, but the amplitudes of the peaks are smaller than that of MD06-3040. Declination of HGY Lake also presents several swings and two of them could be also partially compared to that of MD06-3040 (swings 2 and 3).

Resolution of Erhai Lake is much lower than the three discussed above, but some features are also recognizable. A clear board high value on declination profile which is nicely corresponds to the swing 2′ of core MD06-3040, but the inclination present different behavior from that of core MD06-3040. The low value of declination at about 1.3 ka coincides with inclination peaks, which could be well matched to that of core MD06-3040. Obvious inclination high values around 3.3 ka, and double peaks between 4.5 ka and 5.5 ka, are comparable to that peaks 3 and 4 of core MD06-3040, while the declination behavior is hardly simply compared at this interval.

To sum up, the PSVs from China and Japan are comparable, both from sediments and archeological materials. PSV of core MD06-3040 could be well compared to archeomagnetic results and those from Biwa Lake and Erlongwan, but with some differences from SCL and Erhai Lake. Differences between these results might possibly due to some local effects.

5.3. East Asia PSV stack

Since most of PSVs in China and Japan are comparable, a PSV stack of East Asia is further established, which could yield a regional magnetic field behavior and minimize some local effects and also be an important reference curve for future paleomagnetic studies and be applied for relative dating. Firstly, adjustments on ages would be carried out to make all the PSVs in the same chronology. For the Holocene sedimentary PSV records, core MD06-3040, SCL and HGY Lake have 8–9 ^{14}C age controls, and most of the features are comparable with no temporal offset, we suppose that the ages of the three PSVs are reliable. While there are only two age controls on Biwa Lake, four age controls on Erlongwan and the dating errors for Erhai are larger, some age adjustments on Biwa Lake, Erlongwan and Erhai Lake based on PSV comparison are acceptable. Latest reported age on K-Ah ash layers is cal. 7340 year (Machida, 2002), which is one hundred years older than the age when Biwa Lake PSV published (cal. 7250 year). In this case, the temporal offsets between Biwa and MD06-3040 could be minimized, which further proves that adjustment on Biwa Lake is feasible.

The archeological data from China and Japan almost share the same changing pattern. Even though there are 100–150 year offset between archeomagnetic PSV result and core MD06-3040, it is hardly to say which age controls are more reliable, since they are obtained by different ways. Therefore, no age adjustment was made on archeomagnetic data.

Since the inclination obtained from sediments would be smaller than expected GAD inclination of that latitude, and the difference between them are different, we prefer process these inclination results by subtracting arithmetic mean value for each core, which is also applied on declination results. There are some missing PSV data between 6.5 and 9 ka of SCL Lake, and with some abrupt variations which are hardly to be compared with other PSV results, so this part is not counted into this stack. Then, all the data are further linearly interpolated in the same time resolution of 20-year. Finally, the stacks of inclination and declination are obtained by averaging the values at each age point and the uncertainties of the stack were also calculated (thick black lines with shadows in Fig. 9). The PSV feature of East Asia is recognizable with five clear inclination peaks and five eastward swings on declination (shown as upward arrows in Fig. 9).

Then the PSV stack is compared to with theoretical PSV curves obtained from geomagnetic models (e.g. Korte et al., 2011; Nilsson et al., 2014) to better understand the geomagnetic field variations. The latest geomagnetic field model is established by Nilsson et al. (2014), which is chosen to be compared here (Fig. 9). Predicted PSV could be obtained from the model by site, and there is no obvious geomagnetic field differences in a regional area (20–40°N, 100–140°E). The center of this area is near the site of core MD06-3040 (Fig. 1), so predicted PSVs (pfm9k.1, pfm9k.1a, pfm9k.1b) with different temporal resolution and different restrictions of core

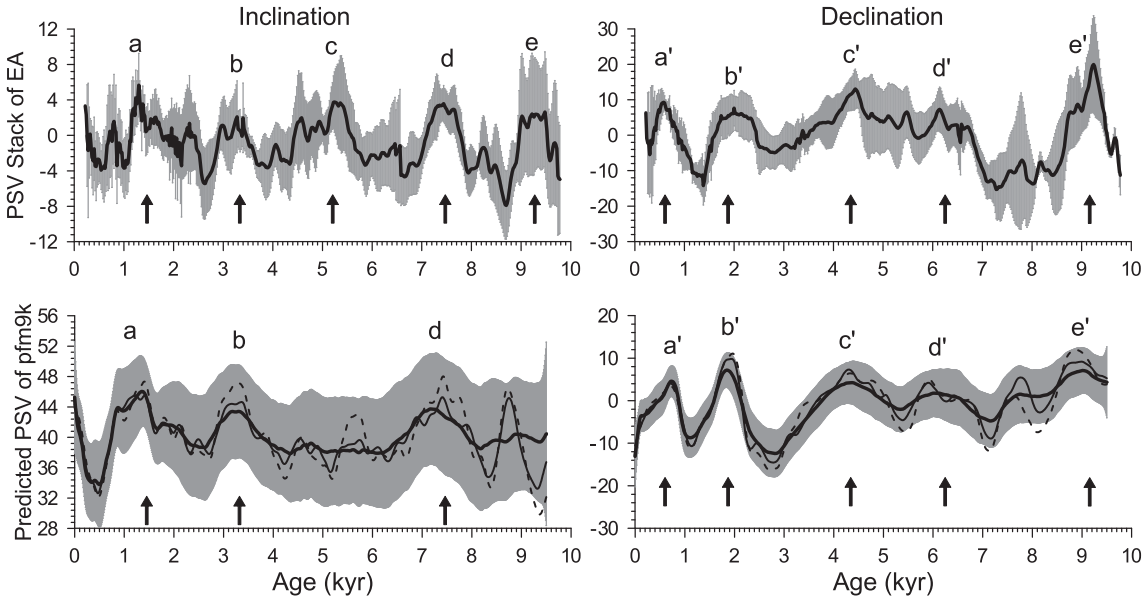

Fig. 9. PSV stack of East Asia (thick black lines—stack; light gray shaded area—95% uncertainty of the stack) with comparison with predicated PSV of East Asia (28°N, 122°E) from geomagnetic field variation model—pfm9k (thick black lines with light gray shaded area—pfm9k.1b; thin black lines-pfm9k.1; thin dots lines-pfm9k1a) (Nilsson et al., 2014).

MD06-3040 are calculated from model and then are compared in Fig. 9. Three inclination peaks and five declination eastward swings can be distinguished from predicted results from models, which are showing similar long-term variation as stack does. The similarity of the two kinds of PSV results proves that the prediction of the model on East Asia is reliable and the stack established by regional real data is convincible.

Some of the features can be well matched each other (inclination peaks b and d, declination swings c′ and e′), and the others shows 100–300 years temporal offset (inclination peaks a, declination swings a′, b, and d′). The ages of PSVs in the stack are constrained by ^{14}C, with limited errors, so the ages of PSV stack is more reliable than that from the model. Furthermore, the uncertainty of pfm9k.1b model on inclination profile is much larger than that of East Asia PSV stack, so we suppose that the regional East Asia stack provide more detailed geomagnetic field information, and could be also used as an important reference curve for relative dating. More well-dated, high-resolution paleomagnetic studies should be carried out in this area, to minimize the uncertainty of the stack and better understand the behavior of the magnetic field.

6. Conclusion

Core MD06-3040 from East China Sea provides a continuous, uniform sedimentary sequence of the upper 18.5 m mud sediments that spans the last 10 ka. Paleomagnetic directions are still preserved by coarse-grained magnetite, even affected by post-depositional diagenetic alteration. Reliable declination and inclination records are obtained from East China Sea, which present six major inclination peaks and five major declination swings. The periodicities for inclination are about 2000 and 550 years, and for declination are about 1400 and 500 years. The PSV of MD06-3040 is comparable to other records from East Asia, to archeomagnetic and historic results of the last 2500 years and to PSV results from lake sediments in southern China and Japan during the Holocene. A PSV stack of East Asia is constructed by sedimentary and archeological PSV results. Similarity long-trend pattern between East Asia PSV stack and that obtained from geomagnetic field models proves that the model prediction is conceivable in this area. The PSV stack provides more detailed magnetic field information with five clear inclination peaks and five eastward declination swings. The stack can be used as a reference curve for a large region, and be potentially applied for correlation between sites and relative dating for sediments of East Asia.

Acknowledgements

The authors sincerely thank IPEV and the crew and staff of MD155-Marco Polo 2-IMAGES XIV cruise on board the R.V. *Marion Dufresne* for providing the samples from MD06-3040. We are grateful to Catherine Kissel and Carlo Laj for their detailed comments on the manuscript. We appreciate the helpful suggestions from two anonymous reviewers. We also thank Andreas Nilsson for providing prediction PSV data sets from pfm9k.1 model, Greig Paterson and Yulong Zhao for data analysis, Camille Wandres and Christine Franke for laboratory assistance, and also thank Guillaume St-Onge, Xiaoqiang Yang, Antti Ojala, and Ian Snowball for sharing their original data sets. This work was jointly supported by the National Natural Science Foundation (NSFC) (Grant No. 41104043, 40830107, 40925012, 40676033), Post-doctoral Foundation (Grant No. 2011M500380) and Ministry of Science and Technology (Grant Nos. 2010DFA24480, 2012CB821900) in China, and by the French Commissariat a l'Energie Atomique (CEA) and the Centre National de la Recherche Scientifique (CNRS).

Appendix A. Supplementary data

Supplementary data associated with this article can be found, in the online version, at http://dx.doi.org/10.1016/j.pepi.2014.07.001.

References

Ali, M., Oda, H., Hayashida, A., Takemura, K., Torii, M., 1999. Holocene palaeomagnetic secular variation at Lake Biwa, central Japan. Geophys. J. Int. 136, 218–228.
Barletta, F., St-Onge, G., Stoner, J.S., Lajeunesse, P., Locat, J., 2010. A high-resolution Holocene paleomagnetic secular variation and relative paleointensity stack from eastern Canada. Earth Planet. Sci. Lett. 298, 162–174.
Brachfeld, S.A., Banerjee, S.K., 2000. A new high-resolution geomagnetic relative paleointensity record for the North American Holocene: a comparison of sedimentary and absolute intensity data. J. Geophys. Res. 105, 821–834.
Cai, S., Tauxe, L., Deng, C., Pan, Y., Jin, G., Zheng, J., Xie, F., Qin, H., Zhu, R., 2014. Geomagnetic intensity variations for the past 8 kyr: new archaeointensity results from Eastern China. Earth Planet. Sci. Lett. 392, 217–229.
Canfield, D.E., Berner, R.A., 1987. Dissolution and pyritization of magnetite in anoxie marine sediments. Geochim. Cosmochim. Acta 51, 645–659.
Clelland, S.-J., Batt, C.M., 2012. Geomagnetic secular variation as recorded in British lake sediments and its application to archaeomagnetic studies. Phys. Earth Planet. Inter. 194–195, 85–97.
Demetrescu, C., Dobrica, V., 2014. Multi-decadal ingredients of the secular variation of the geomagnetic field. Insights from long time series of observatory data. Phys. Earth Planet. Inter. 231, 39–55.
Frank, U., 2007. Palaeomagnetic investigations on lake sediments from NE China: a new record of geomagnetic secular variations for the last 37 ka. Geophys. J. Int. 169, 29–40.
Gogorza, C.S.G., Sinito, A.M., Tommaso, I.D., Vilas, J.F., Creer, K.M., Nunez, H., 2000. Geomagnetic secular variations 0–12 kyr as recorded by sediments from Lake Moreno (southern Argentina). J South Am. Earth Sci. 13, 627–645.
Heirtzler, J.R., Nazarova, K., 2003. Geomagnetic secular variation in the Indian Ocean. Earth Planet. Sci. Lett. 207, 151–158.
Hervé, G., Chauvin, A., Lanos, P., 2013. Geomagnetic field variations in Western Europe from 1500BC to 200AD. Part I: Directional secular variation curve. Phys. Earth Planet. Inter. 218, 1–13.
Hyodo, M., Yoshihara, A., Kashiwaya, K., Okimura, T., Masuzawa, T., Nomura, R., Tanaka, S., Tang, B.X., Liu, S.Q., Liu, S.J., 1999. A late Holocene geomagnetic secular variation record from Erhai Lake, southwest China. Geophys. J. Int. 136, 784–790.
Jackson, A., Jonkers, A.R.T., Walker, M.R., 2000. Four centuries of geomagnetic secular variation from historical records. Phil. Tran. R. Soc. Lond. A 358, 957–990.
Korhonen, K., Donadini, F., Riisager, P., Pesonen, L.J., 2008. GEOMAGIA50: an archeointensity database with PHP and MySQL. Geochem. Geophys. Geosyst. 9, Q04029.
Korte, M., Constable, C., Donadini, F., Holme, R., 2011. Reconstructing the Holocene geomagnetic field. Earth Planet. Sci. Lett. 312, 497–505.
Laj, C., on board party, 2006. MD155-Marco Polo 2 IMAGES XIV cruise report, des rapports de campagnes à la mer. IPEV.
Lhuillier, F., Fournier, A., Hulot, G., Aubert, J., 2011. The geomagnetic secular-variation timescale in observations and numerical dynamo models. Geophys. Res. Lett. 38, L09306.
Liu, J., Xu, K., Li, A., Milliman, J., Velozzi, D., Xiao, S., Yang, Z., 2007. Flux and fate of Yangtze River sediment delivered to the East China Sea. Geomorphology 85, 208–224.
Lougheed, B.C., Snowball, I., Moros, M., Kabel, K., Muscheler, R., Virtasalo, J.J., Wacker, L., 2012. Using an independent geochronology based on palaeomagnetic secular variation (PSV) and atmospheric Pb deposition to data Baltic Sea sediments and infer ^{14}C reservoir age. Quat. Sci. Rev. 42, 43–58.
Lund, S.P., 1996. A comparison of Holocene paleomagnetic secular variation records from North America. J. Geophys. Res. 101, 8007–8024.
Machida, H., 2002. Volcanoes and tephras in the Japan area. Global Environ. Res. 6, 19–28.
Nilsson, A., Holme, R., Korte, M., Suttie, N., Hill, M., 2014. Reconstructing Holocene geomagnetic field variation: new methods, models and implications. Geophys. J. Int. 198, 229–248.
Ojala, A.E.K., Saarinen, T., 2002. Palaeosecular variation of the Earth's magnetic field during the last 10,000 years based on the annually laminated sediment of Lake Naut jarvi, central Finland. Holocene 12, 393–402.
Ojala, A.E.K., Tiljander, M., 2003. Testing the fidelity of sediment chronology: comparison of varve and paleomagnetic results from Holocene lake sediments from central Finland. Quat. Sci. Rev. 22, 1787–1803.
Qin, Y.S., Zhao, Y.Y., Chen, L.R., Zhao, S.L., 1987. Geology of the East China Sea. Science Press, Beijing.
Schulz, M., Stattegger, K., 1997. SPECTRUM: spectral analysis of unevenly spaced paleoclimatic time series. Comp. Geosci. 23, 929–945.
Skinner, L.C., McCave, I.N., 2003. Analysis and modelling of gravity- and piston coring based on soil mechanics. Mar. Geol. 199, 181–204.
Smirnov, A.V., 2006. Memory of the magnetic field applied during cooling in the low-temperature phase of magnetite: grain size dependence. J. Geophys. Res. 111, B12S04.

Snowball, I., Zillen, L., Ojala, A., Saarinen, T., Sandgren, P., 2007. FENNOSTACK and FENNORPIS: varve dated Holocene palaeomagnetic secular variation and relative palaeointensity stacks for Fennoscandia. Earth Planet. Sci. Lett. 255, 106–116.

Stoner, J.S., Jennings, A., Kristjánsdóttir, G.B., Dunhill, G., Andrews, J.T., Hardardóttir, J., 2007. A paleomagnetic approach toward refining Holocene radiocarbon-based chronologies: paleoceanographic records from the north Iceland (MD99-2269) and east Greenland (MD99-2322) margins. Paleoceanography 22 (1), PA1209.

St-Onge, G., Stoner, J.S., Hillaire-Marcel, C., 2003. Holocene paleomagnetic records from the St. Lawrence Estuary, eastern Canada: centennial- to millennial-scale geomagnetic modulation of cosmogenic isotopes. Earth Planet. Sci. Lett. 209, 113–130.

Yamazaki, T., Abdeldayem, A.L., Ikehara, K., 2003. Rock-magnetic changes with reduction diagenesis in Japan Sea sediments and preservation of geomagnetic secular variation in inclination during the last 30,000 years. Earth Planets Space 55, 327–340.

Yang, S., Odah, H., Shaw, J., 2000. Variations in the geomagnetic dipole moment over the last 12000 years. Geophysical Journal International 140, 158–162.

Yang, X., Heller, F., Yang, J., Su, Z., 2009. Paleosecular variations since ~9000 yr BP as recorded by sediments from maar lake Shuangchiling, Hainan, South China. Earth Planet. Sci. Lett. 288, 1–9.

Yang, X., Liu, Q., Duan, Z., Su, Z., Wei, G., Jia, G., Ouyang, T., Su, Y., Xie, L., 2012. A Holocene palaeomagnetic secular variation record from Huguangyan maar Lake, southern China. Geophys. J. Int. 190, 188–200.

Zheng, Y., Kissel, C., Zheng, H., Laj, C., Wang, K., 2010. Sedimentation on the inner shelf of the East China Sea: magnetic properties, diagenesis and paleoclimate implications. Mar. Geol. 268, 34–42.

Zijderveld, J.D.A., 1967. AC demagnetization of rock: analysis of results. In: Collinson, D.W., Creer, K.M., Runcorn, S.K. (Eds.), Methods in Paleomagnetism. Elsevier, Amsterdam, The Netherlands, pp. 254–286.